Lifetime of the $^{18}O\ 4_1^+$ state at 3.555-MeV excitation

J. P. Coffin, A. Gallmann, F. Haas, P. Wagner, and J. W. Olness*
Centre de Recherches Nucléaires et Université Louis Pasteur, Laboratoire de Physique Nucléaire et d'Instrumentation Nucléaire, 67037-Strasbourg-Cedex, France

(Received 18 September 1973)

The recoil distance method was used to measure the lifetime of the $J^\pi = 4^+$ second excited state of ^{18}O at 3.555-MeV excitation, which was formed via the $^{16}O(t,p)^{18}O^*$ reaction at $E_t = 3.1$ MeV. The mean life is found to be $\tau = 46.2 \pm 3$ psec, which corresponds to an $E2$ strength for the 3.55 $(4^+) \rightarrow 1.98$ (2^+) transition of $|M(E2)|^2 = 0.64 \pm 0.05$ Weisskopf units. This result is in good agreement with the predictions of recent theoretical calculations in the weak-coupling model, which identifies the lowest-lying 2^+ and 4^+ states as predominantly 2p-0h states based on ^{16}O. The predictions of this model for mirror states ^{18}O-^{18}Ne are discussed. Additional data were obtained coincidentally for states of ^{18}F formed via the competing $^{16}O(t,n)^{18}F^*$ reaction. The results, which are in good agreement with previous values, are: 0.937-MeV state, $\tau = 65.4 \pm 5.3$ psec and for the 1.081-MeV state, $\tau = 26.1 \pm 2.3$ psec.

I. INTRODUCTION

Extensive theoretical calculations for $A = 16$–19 nuclei, based on a formulation of particle-hole states in the weak-coupling model, have recently been reported by Engeland and Ellis.[1] Their results, which are in good agreement with comparable earlier calculations by Benson and Flowers[2] and Zuker, Buck, and McGrory,[3] have been quite successful in explaining not only the observed level structure, but also the experimentally determined spectroscopic factors and γ-ray decay modes of these nuclei. A comprehensive comparison of theory and experiment has been given in their article,[1] which includes the data available then (in 1971) on the mass-18 triad ^{18}O-^{18}F-^{18}Ne.

More recently additional information on ^{18}O has been reported[4] from measurements of lifetimes in the $^{19}F(t,\alpha\gamma)^{18}O$ reaction via the Doppler-shift-attenuation method (DSAM). As a consequence of these studies[4] it was determined that 14 of the 15 levels below 7.2-MeV excitation in ^{18}O have mean lives $\tau \lesssim 3.5$ psec. The exception noted is for the second excited state at 3.555 MeV ($J^\pi = 4^+$) which decays by a 100% branch to the first excited state at 1.982 MeV ($J^\pi = 2^+$). The lifetime in this case was too long for a DSAM measurement, and only a lower limit $\tau > 4$ psec was obtained, compared to the weak-coupling prediction[1] which is $\tau = 23$ psec. On the other hand the lifetime of the analog 4^+ state in the mirror nucleus ^{18}Ne has been reported[5] as 4.4 ± 0.6 psec.

In view of the previous experimental restriction $\tau > 4$ psec we have selected the recoil-distance method (RDM) to measure this lifetime, using the $^{16}O(t,p)^{18}O^*$ reaction ($Q = 3.707$ MeV[6]) to form the initial ^{18}O state. The reaction is appropriate here since the effective Q for the 3.55-MeV state is only 0.16 MeV, and thus the kinematics insure that the excited ^{18}O recoil ions are moving in a forward cone of maximum angle $\theta_R < 30°$. Moreover the competing $^{16}O(t,n)^{18}F^*$ reaction ($Q_0 = 1.270$ MeV) provides several useful calibrations for the RDM measurement, since ^{18}F is known[6] to have several low-lying states with lifetimes in the psec range.

Figure 1 summarizes the excitation energies, lifetimes, and major decay modes of those states of ^{18}O and ^{18}F which are of interest here. It is worthwhile to note that the higher-lying states of ^{18}O which might be formed directly in the (t,p) reaction and cascade through the 3.55-MeV level all have lifetimes appreciably shorter than the limit $\tau > 4$ psec, and thus feeding of the 3.55-MeV state via cascade radiations will not seriously perturb the RDM measurement.

A description of the experimental method and results is given in Sec. II, and a brief discussion is appended in Sec. III, which includes a comparison of the mirror transitions in ^{18}O-^{18}Ne.

II. EXPERIMENT

A. Procedure

The reactions $^{16}O(t,p)^{18}O^*$ and $^{16}O(t,n)^{18}F^*$ were initiated by 3.1-MeV triton bombardment of a target of natural silica made up of a 90-μg/cm^2 layer of SiO_2 evaporated onto a 0.8-mg/cm^2 nickel foil. The particular apparatus used for the RDM measurement has been described in detail previously.[7,8]

γ rays were detected at 0° relative to the beam direction by a 100-cm^3 Ge(Li) detector located

8.6 cm from the target. The intrinsic resolution of the detector system was 3.3 keV for 1.332-MeV γ rays. Energy calibration was based on the many ^{18}O and ^{18}F lines in the experimental spectra, together with additional lines resulting from (t,p), (t,n), and (t,α) reactions on the $^{58,60}Ni$ target backing.

Measurements were made for several distances corresponding to $D<200$ μm, where D is the measured distance between the target foil and the stopper. An additional "background" measurement was made at $D=1000$ μm. The typical running time for these measurements was ~3 h at a beam current of 30 nA.

Figure 2 shows a portion of the data recorded for $D=90$ μm, illustrating the line shapes measured for the ^{18}O 3.555 $(4^+)\rightarrow$ 1.982 (2^+) transition, and also the 0.937 $\rightarrow$ 0 and 1.081 $\rightarrow$ 0 transitions in ^{18}F. The solid curve in each case illustrates a least-squares fit to the data, which was carried out to determine the intensities of the *fast* and *stopped* components, I_s and I_0, which correspond, respectively, to the Doppler-shifted transitions from nuclei which decay in flight (I_s) and the unshifted transitions from nuclei which decay at rest (I_0), i.e., after reaching the stopper.

The individual line shapes were represented by the sum of two Gaussian peaks, of different widths, superimposed on a smooth background given by the dashed lines. The shaded area shows the intensity of the unshifted peak measured for $D=1000$ μm, at which distance the lifetime of these states would require that $I_0 \cong 0$. There are three possible sources for this residue: (a) All of the nickel foils tested had an oxide contamination, most likely in the form of a surface layer of nickel oxide. The net result is that ^{18}F and ^{18}O ions produced in the oxide layer on the beam side of the Ni foil are stopped rapidly, giving rise to a component of I_0 which is obviously independent of plunger distance D. (b) Large-angle scattering of the less energetic excited nuclei can result in a small fraction of nuclei (from the SiO_2 target) whose velocity component along the beam axis is ~0. (c) The state in question may be partially fed by γ cascade from higher-lying states of much longer lifetime.

In the case of the ^{18}O 3.555 $\rightarrow$ 1.982 and ^{18}F 1.081 $\rightarrow$ 0 transitions there are no higher-lying states of significantly long lifetime, and thus the observed

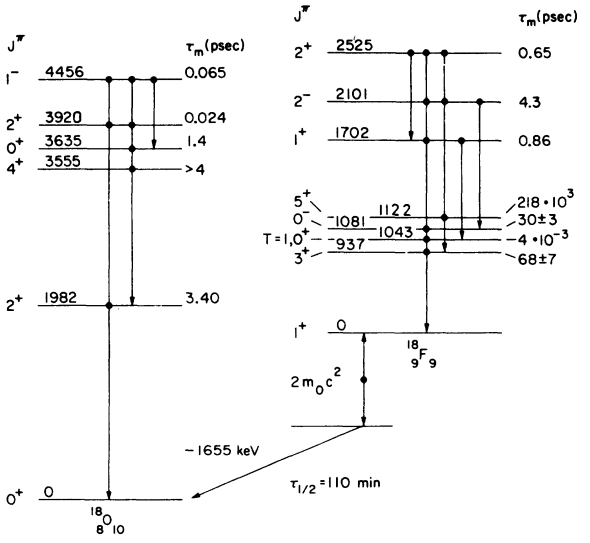

FIG. 1. Lifetimes and γ branching for low-lying states of ^{18}O and ^{18}F. The lifetimes are those given in Ref. 4 (for ^{18}O) and Ref. 6 (for ^{18}F).

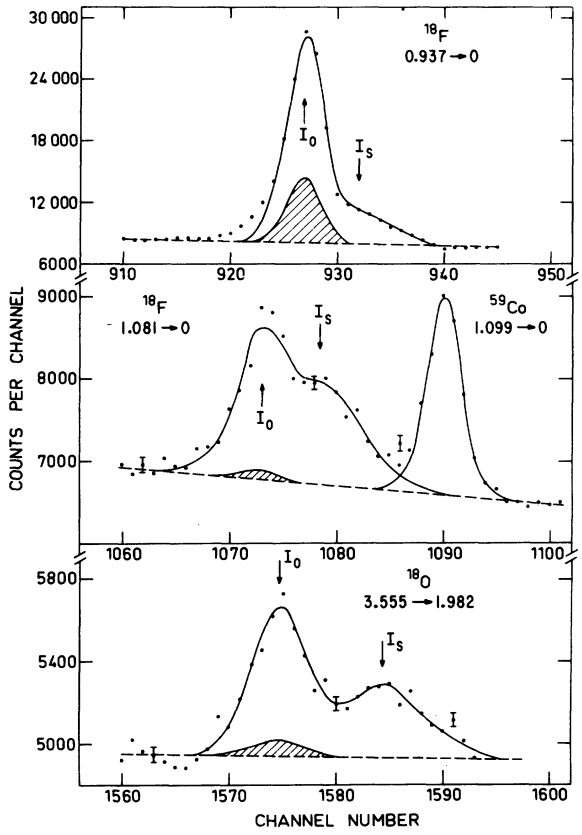

FIG. 2. Portions of a Ge(Li) spectrum at $\theta_\gamma=0^0$ illustrating line shapes measured for deexcitation of those states in ^{18}F and ^{18}O formed via the (t,n) and (t,p) reactions on ^{16}O. These data were taken at a target-stopper distance $(D-D_0)=55$ μm. The solid curves in each case are the results of a computer fit to determine the intensities of the shifted and stopped components, whose centroids are labeled I_s and I_0, respectively. Also seen in these data is the ground-state decay of a state in ^{59}Co populated via the (t,α) reaction on the nickel backing of the SiO_2 target. The dispersion is 0.984 keV/channel.

effect is a combination of (a) and (b). In both cases, the residue peak at $D = 1000$ μm is 6% of the total intensity, and provides a measure of these two effects. For the ^{18}F 0.937→0 transition, the residue at $D = 1000$ μm is ~23% of the total intensity: The difference (23-6) = 17% corresponds to the feeding of the 0.937-MeV state from the longer-lived 1.122-MeV state. Since the latter lifetime is $\tau = 218 \times 10^3$ psec, its contribution will not vary over the 1000 μm of the measurement. After subtraction of the residues the ratios $R = I_0/(I_0 + I_s)$ were constructed, and are plotted in Fig. 3.

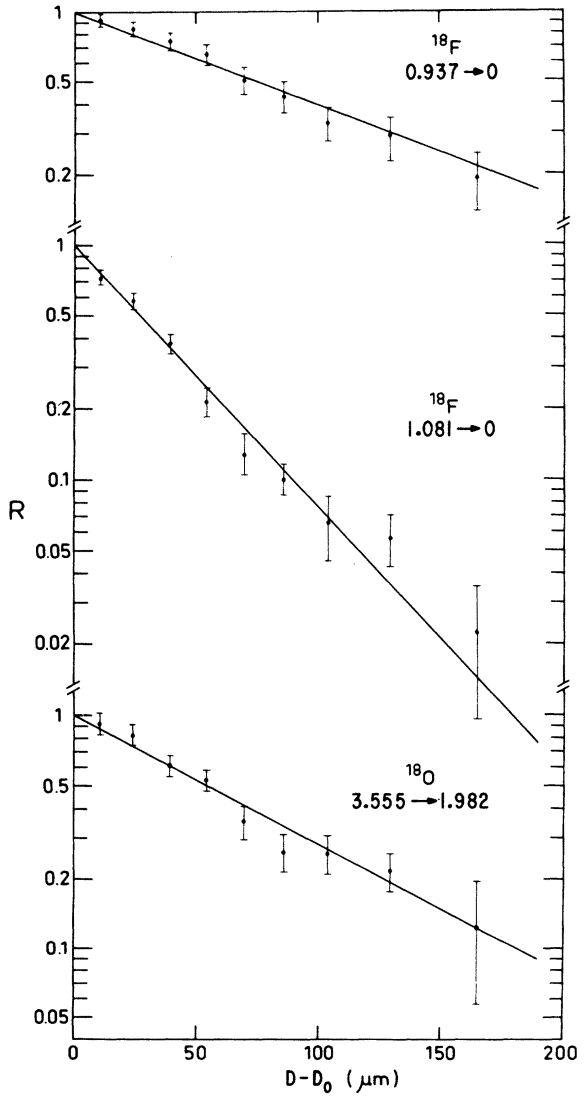

FIG. 3. The experimental ratios $R = I_0/(I_0 + I_s)$ plotted as a function of target-stopper distance D-D_0, with $D_0 = 35$ μm. The solid curves are the results of a computer fit to determine the lifetime of the initial states in ^{18}F and ^{18}O.

B. Analysis and results

The general procedure of analysis, including a discussion of the various geometrical corrections which must be applied to R, is discussed in detail in Refs. 7, 8, and 9. Corrections due essentially to the different solid angles for detection of I_0 and I_s are small, because of the large target-detector distance, and low recoil velocities ($v/c < 0.6\%$). Of major importance however is the distribution of recoil velocities. In the present case the width of this distribution is comparable to the mean velocity itself. Since we find that the velocity distribution is well represented by a Gaussian distribution we chose to analyze the data in terms of an analytic representation

$$R = \int f(v - v') e^{-(D - D_0)/v'\tau} dv' .$$

Here v is the mean recoil velocity (z component) and D_0 is the measured value for true zero distance. The integration is to be carried out over the range of actual velocities $0.05 \leq v'$ (μm/psec) ≤ 3.40 corresponding to the Gaussian distribution function $f(v - v')$.

A preliminary fit to all three sets of data (Fig. 3) with D_0 taken as a parameter of the fit established a unique solution $D_0 = 35$ μm. This value was then adopted and fixed for the final fit, shown in Fig. 3. The results for τ and also the mean values of the velocity distribution v, are summarized in Table I. Also shown for comparison are the results obtained by setting $v' \equiv v$; i.e., assuming a velocity distribution of zero width.

As a final check on the procedures of analysis, the velocity distribution was calculated for an assumed isotropic distribution in the (t, p) and (t, n) reactions. In calculating the effective z component of velocity, account was taken of the ion energy loss in the SiO_2 target layer and the effect of the finite solid angle of the γ-ray detector. The resultant velocity distribution, when folded with a Gaussian representing the detector resolution function of width, reproduces the observed width to within ~10%. The mean velocities are ~9% high compared to the experimental values for v listed

TABLE I. Lifetime results for ^{18}O and ^{18}F.

Transition	v (μm/psec)	τ_m (psec) Present (Without) [a]	(With) [a]	Previous [b]
^{18}F 0.937→0	1.600±0.097	60.0±4.0	65.4±5.3	68±7
^{18}F 1.081→0	1.495±0.110	28.0±2.7	26.1±2.3	30±3
^{18}O 3.555→1.982	1.700±0.057	43.6±2.5	46.2±3.0	•••

[a] Results are given as obtained with and without the velocity distribution correction discussed in the text.
[b] Results summarized in Ref. 6.

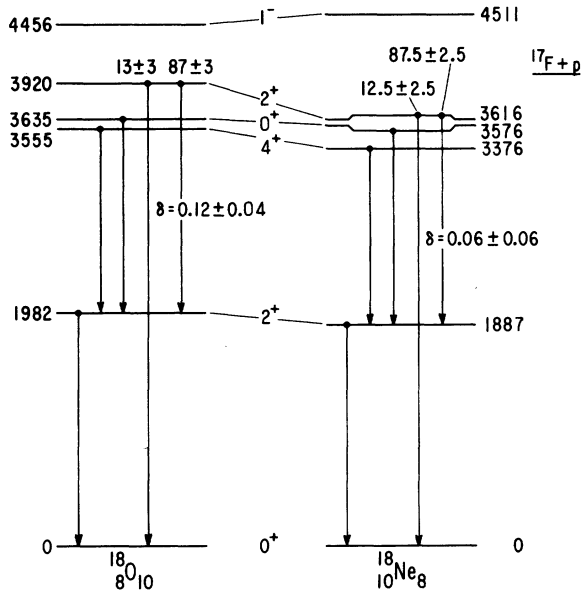

FIG. 4. Excitation energies, branching rations, and multipole mixing ratios for mirror states of $A=18$. The data are taken from Ref. 4 (^{18}O) and Refs. 5 and 6 (^{18}Ne). In particular, the branching ratios and multipole mixing ratios for the ^{18}Ne 3.616-MeV state are those summarized in Ref. 5.

in Table I. This can be tentatively accounted for in terms of the expected slight forward peaking of the (t,p) and (t,n) reactions, coupled with the fact that some fraction of the feeding of the states in question arises from cascades from higher-lying states for which Q is negative. It is felt significant that the agreement in individual cases is within the uncertainties in v (and also τ) as given in Table I, which result we take as partial justification for the method of analysis given.

III. SUMMARY AND DISCUSSION

With reference to Table I we note that our results for ^{18}F lifetimes are in excellent agreement with the previous values.

Our experimental result for the ^{18}O 4^+ state can now be combined with previous results[4-6] to allow a more complete comparison of the mirror correspondences for ^{18}O-^{18}Ne. Figure 4 illustrates the states of interest here; note that in ^{18}Ne, states of excitation energy $E_x > 3.922$ are unbound against proton emission. Table II summarizes experimentally determined $E2/M1$ strengths for the decay of these lowest-lying even-parity states. Strengths are given in the conventional Weisskopf units (W.u.). The source of the various lifetime measurements, as well as branching and mixing ratios, is specifically indicated. With respect to future experimental interest, we note that the value given for the mean life of the ^{18}Ne 3.576 state is taken[5] as the central value between the experimentally defined limits $2 \leq \tau$ (psec) ≤ 6. The value measured[5] via the RDM for the 3.376-MeV level, $\tau = 4.4 \pm 0.6$ psec, is not in very good agreement with the value previously reported[10] from DSAM measurements, $\tau = 1.9^{+1.0}_{-0.4}$ psec. The RDM measurement should in principle be more accurate, and has been adopted in Table II. However, further experimental checks on these two lifetimes are clearly desirable.

TABLE II. Summary of lifetime measurements and transition strengths for ^{18}O and ^{18}Ne.

Nucleus	Transition	J_i^π, J_f^π	Multipole	τ_m (psec)	$\lvert M\rvert^2$ (in W.u.) Exp [a]	Theory [b]
^{18}O	1.982 → 0	$2^+, 0^+$	$E2$	3.40 ± 0.26 [c]	2.74 ± 0.21	1.8
	3.555 → 1.982	$4^+, 2^+$	$E2$	46.2 ± 3	0.64 ± 0.05	1.3
	3.635 → 1.982	$0^+, 2^+$	$E2$	1.40 ± 0.14 [c]	16.5 ± 1.6	3.3
	3.921 → 0	$2^+, 0^+$	$E2$	0.024 ± 0.010 [c]	1.7 ± 0.8	1.7
	→ 1.982	$2^+, 2^+$	$M1$		0.15 ± 0.06	0.07
			$E2$		$5.3^{+4.6}_{-3.7}$	1.3
^{18}Ne	1.887 → 0	$2^+, 0^+$	$E2$	$0.49^{+0.17}_{-0.09}$ [d]	24 ± 6	11.5
	3.376 → 1.887	$4^+, 2^+$	$E2$	4.4 ± 0.6 [e]	8.8 ± 1.2	9.4
	3.576 → 1.887	$0^+, 2^+$	$E2$	4 ± 2 [e]	5.2 ± 1.6	1.2
	3.616 → 0	$2^+, 0^+$	$E2$	$0.063^{+0.030}_{-0.020}$ [d]	0.9 ± 0.4	0.45
	→ 1.887	$2^+, 2^+$	$M1$		0.08 ± 0.03	0.06
			$E2$		1^{+3}_{-1}	7.9

[a] For the decay of the second excited 2^+ states, the mixing ratios and branching ratios are those of Refs. 4 and 5, as given in Fig. 4.

[b] See Ref. 1.

[c] See Ref. 4.

[d] See Ref. 10.

[e] See Ref. 5.

The weak-coupling-model predictions of Engeland and Ellis[1] are given for comparison; in this case (mass 18) the 0h-2p and 2h-4p configurations are specifically $(sd)^2$ and $p^{-2}(sd)^4$, respectively. As has been discussed previously[1,4,5] the agreement between theory and experiment is reasonably good. The lowest-lying 2^+ and 4^+ states in ^{18}O-^{18}Ne are expected[1] to be essentially pure 0h-2p states, in which case the ratio of mirror $E2$ transitions (^{18}O/^{18}Ne) should be ~9, as given by the factor $[(1+\beta)/\beta]^2$ with an effective polarization charge $\beta e = 0.5e$. The experimental ratios are 8.8 for the first 2^+ states, and 13.3 for the 4^+ states; for comparison, the model predictions are 6.6 and 7.3, respectively. For the higher-lying 0^+ and 2^+ states the ratios are unity, which as remarked previously,[5] is in agreement with the 2h-4p nature of these states.

A comparison can be made between the decay modes of the 4^+ states in the $A=18$ triad. The γ decay of the analog 4^+ state in ^{18}F (isobaric quantum number $T_3=0$) has been recently investigated by Rolfs, Berka, and Azuma,[11] who set a limit on the mean lifetime $\tau<10$ fsec. The observed decay takes place via $\Delta T=1$ transitions to lower-lying states of ^{18}F, and an upper limit of <1.2% is placed on the branching ratio of the analog $4^+ \rightarrow 2^+$ ($\Delta T=0$) transition. Since the $E2$ strength for an isobaric state of given T_3 may be simply expressed in terms of the isoscalar and isovector components $|M(E2)|^2 = |M_s + T_3 M_v|^2$, the measured $E2$ strengths for ^{18}O and ^{18}Ne ($T_3=+1$ and -1, respectively) may be used to obtain the ^{18}F $T_3=0$ strength. The result is

$$|M(E2)|^2 = 3.6 \text{ or } 1.2 \text{ W.u.}$$

The isoscalar and isovector amplitudes are clearly of comparable magnitude but of opposite phase. If we combine the larger value for ^{18}F, $|M(E2)|^2 = 3.6$ W.u., with the lifetime restriction $\tau<10$ fsec, we obtain the restriction on the $4_1^+ \rightarrow 2_1^+$ branching ratio $\Gamma_{E2}/\Gamma_{\text{total}} < 0.13\%$, which is yet compatible with the experimental limit of <1.2%.

---

*Visitor. Permanent address: Brookhaven National Laboratory, Upton, N.Y. 11973.

[1]T. Engeland and P. J. Ellis, Nucl. Phys. A181, 368 (1972).
[2]H. G. Benson and B. H. Flowers, Nucl. Phys. A126, 332 (1969).
[3]A. P. Zuker, B. Buck, and J. B. McGrory, Phys. Rev. Lett. 21, 39 (1968); A. P. Zuker, *ibid.* 23, 983 (1969); J. B. McGrory, Phys. Lett. 31B, 339 (1970).
[4]J. W. Olness, E. K. Warburton, and J. A. Becker, Phys. Rev. C 7, 2239 (1973).
[5]R. D. Gill, J. M. G. Caraça, A. J. Cox, and H. J. Rose, Nucl. Phys. A180, 79 (1972).
[6]F. Ajzenberg-Selove, Nucl. Phys. A190, 1 (1972).
[7]K. W. Jones, A. Z. Schwarzschild, E. K. Warburton, and D. B. Fossan, Phys. Rev. 178, 1773 (1969).
[8]A. Gallmann, G. Frick, B. Heusch, F. Haas, and E. K. Warburton, Nucl. Phys. A143, 326 (1970).
[9]D. B. Fossan and E. K. Warburton, in *Nuclear Spectroscopy II*, edited by J. Cerny (Academic, New York, to be published).
[10]B. C. Robertson, R. A. I. Bell, J. L'Ecuyer, R. D. Gill, and H. J. Rose, Nucl. Phys. A126, 431 (1969).
[11]C. Rolfs, I. Berka, and R. E. Azuma, Nucl. Phys. A199, 306 (1973). Further references for F^{18} are cited therein.